Shinshu University Journal of Educational Research and Practice, No.5, pp.83-94, 2012
信州大学教育学部研究論集　第5号　pp.83-94　2012年

<Academic paper>

Relationship Between the Nocturnal Heat Island and Inversion Layer in Matsushiro, Nagano

SAKAKIBARA Yasushi **Faculty of Education, Shinshu University**
HOJO Makie **Miyota Minami Elementary School, Nagano**
NAKAGAWA Kiyotaka **Faculty of Geo-Environmental Science, Rissho University**

Keywords: heat island, rural lapse rate, wind speed, Matsushiro, city size

1. Introduction

The population of the cities increase and the urban surface was covered by the concrete and asphalt, when the cities develop. As a result, the heat balance at the urban surface changed and the temperature of the city became higher. This phenomenon was called 'heat island', which brought about the hot summer night when the people can not sleep well without the air conditioning.

It is important to understand the physical process and the cause of heat island for the measure. The city was regarded as the flat slab in the previous numerical model for simulation. Recently the elaborate numerical model with an urban canopy model was developed (ex. Kusaka and Kimura, 2004). But many models do not attain the practical use level. To forecast the growth of heat island since there were many challenges such as production of data set about surface parameter, soil temperature and so on in actual cities.

Oke (1973) showed that there was the linear relation between the yearly maximum of heat island intensity (*HII*) and the logarithm of population to explain the development of heat island by the city size. The heat island appearance was expressed with only parameter of city population in this empirical model with high coefficients of determination of 0.96. But this model is applicable only in a ideal condition when heat island develops well.

Generally speaking heat island appears well in a calm and fine night. Rural surface inversion layer develops well in the same condition. Tamiya and Ohyama (1981) reported that the larger the rural lapse rate (*RLR*), the larger the *HII*. In addition, they presented the model that the heat island resulted from the mechanical mixing of the ground air and warmer air aloft by the urban larger roughness, when rural air went in and traveled the urban area. And they showed *HII* was in proportion to *RLR*.

Summers (1965) discussed the relationship between the strength of surface inversion and *HII* theoretically. He developed a heat island model that considers changes in the stable air moving

across an urban area, which may act as a heat source. His result showed that the *HII* was proportional to the square root of (*RLR* / rural windspeed).

Recently observational result showed that the correlation coefficient between *HII* and *RLR* was larger than that between *HII* and the square root of (*RLR* / rural wind speed) (Tamiya and Ohyama,1981; Sakakibara, 1998; Sakakibara, 2001).

Ludwig (1974) tried to generalize the relationship between *HII* and *RLR* based on published data. He divided 12 cities into 3 groups such as small cities, middle cities and large cities. The regression line of each group was calculated. He showed that the gradient of regression line became larger in the bigger cities. His results stressed this method the practical significance. However, no cities with populations less than 30,000 were included in his sample, and thus it is unclear whether the classification system applies to smaller cities. If this theory is true, the gradient in smaller cities ought to be smaller.

We have studied *RLR* as a predictor of heat island. Temperature distributions were observed in and around a smaller city, and pseudovertical temperature profiles were taken in rural areas to study a screen level heat island. This paper confirms Ludwig's study and discusses whether his theory is applicable in the wider range of city size.

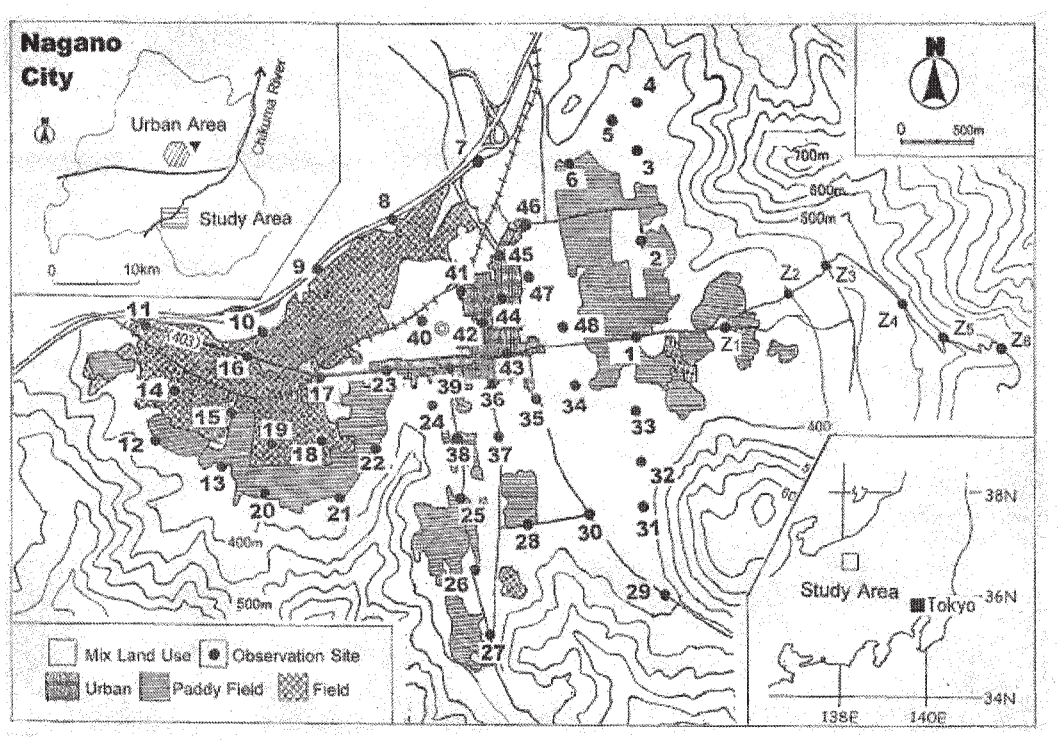

Fig. 1. Map of the study area.
◎:Matsushiro Observatory, ▼:Nagano Local Meteorological Observatory, ●: observation stations, [Z_1] - [Z_6] :observation stations for inversion layer .

2. Research area

We conducted this study in Matsushiro Town, a small town that is part of Nagano City in Nagano Prefecture, Japan (Fig. 1). The town is 10 km south of downtown Nagano, and the 2002 census recorded a population of 20,430. This town is under the same political administration as Nagano City. However, we regarded these settlements as different because they are separated by the Chikuma River. Downtown Matsushiro is approximately 350 m in altitude. There is a flat land north of the town, but mountains in other directions. Route 403 passes through the center of town. This road can have somewhat heavy vehicle traffic in daytime but has almost no traffic at night. Of the field survey points, we selected points 41-45 to represent the urban area. This area had many three- to four-story buildings. Point 43 was the largest building-land ratio point in all observation points. The value was 0.85 and the sky view factor was 0.79. We selected points 12-16 and 18-22 to represent rural sites. These areas had typical rural landscapes of agricultural fields and rice paddies. Point 19 was the smallest the building-land ratio point in all observation points. The value was 0 and the sky view factor was 0.94. A paddy field was also located near point 4. However, we did not include this point in the rural data set because buildings had been constructed on parts of the field. The paddy fields were flooded at the end of May, and drained beginning in September according to the maturity level of the rice. Rice was harvested in October, leaving the paddy fields bare.

Annual mean temperature in this area was 11.7 ℃ and annual range of temperature was 25.6 ℃ and larger than that in many Japanese cities. Monthly mean temperature was -1.2 ℃ in January. Annual amount of precipitation was 938 mm/year. We had mach precipitation in Summer.

3. Method

3.1 Observation method

Forty-eight points along a paved road in Matsushiro were selected as observational points (Fig. 1). Air temperatures were measured as the car moved in numerical order of the observation points. A thermometor (Hioki EE Corp., Ueda, Japan, 9021-01) was used as the temperature sensor and was accurate within ± 0.2℃. Because measurements were taken as the car moved at 10 m/s, the movement of the car ventilated the system; thus, no other ventilation system was necessary. The time constant was within 10 s at this wind speed.

The sensor was connected to a handheld computer (Seiko-Epson, Suwa, Japan, HC-40). It was held in a radiation shield constructed of a polyvinyl chloride (PVC) tube (107 mm diameter, 3 mm thick, 360 mm long). The radiation shield was covered with an aluminum sheet to avoid heating by radiation, and connected to another PVC tube (80 mm diameter, 3 mm thick, 3200 mm long), which was fastened to a roof-top carrier on the automobile, thus fixing the

radiation shield tube 150 cm above the ground over the edge of the automobile fender. In this position, engine heat was less likely to influence the measurements (Sahashi, 1983).

Observations along the entire route took approximately 50 min. Time correction was done assuming that the temperature variation at all points were the same as that at point 1. We conducted 70 nocturnal temperature surveys, each lasting a few hours, on clear and cloudy evening from 5 December 2001 to 15 November 2002 (Table 1). It appears in table 1 that all surveys were conducted under near-calm or light breeze conditions (under 2 m/s). Wind was not a strong heat island control during any of the observation nights.

Observation points were generally at 350 m altitude, but observations at points 18-32 were 40 m higher than other observations. Comparing fine and cloudy days, no differences in the influence of altitude was shown in the temperature distributions. This effect of height difference on tempreratures was ignored owing to a small height difference.

Table 1 Meteorological condition

No	Date	Horizontal Obs.Time	Vertical Obs.Time	Cloud	Matsusiro Obsevatory Hour	U(m/s)		NLO Sun
1	011205	2223-2306	2216-2222	6	23	0.9	S	4.8
2	011211	2212-2259	2205-2211	2	23	0.9	SSW	5
3	011218	2146-2233	2139-2146	0	22	1.2	S	3.6
4	011223	2241-2316	2232-2240	0	23	0.1	C	8.6
5	020112	2201-2249	---	9	22	0.7	NNW	8.2
6	020114	2237-2321	---	1	23	1	S	8.7
7	020117	2138-2227	2128-2136	1	22	1.9	NE	1
8	020123	2159-2249	2149-2156	10	22	0.8	SSW	2.2
9	020125	2210-2258	2121-2210	0	23	0.9	S	1.5
10	020201	2152-2238	---	1	22	0.3	WNW	9.4
11	020202	2151-2234	2151-2202	10	22	0.1	C	5.8
12	020206	2143-2233	---	0	22	1.1	SSE	8.9
13	020208	2254-2339	2246-2251	0	23	0.8	SW	5.2 *
14	020227	2149-2240	---	6	22	1.7	ENE	3.5
15	020303	2150-2235	2158-2204	2	22	1.2	ENE	8.4
16	020304	2150-2237	2143-2149	0	22	0.9	WSW	11
17	020309	2146-2235	2140-2145	0	22	0.9	S	11
18	020311	2144-2231	2136-2144	1	22	1.3	SSW	9.4
19	020316	2137-2226	2131-2137	0	22	0.9	SSW	6.5
20	020321	2141-2237	2134-2141	10	22	1.8	NE	5.4
21	020322	2239-2329	2233-2239	---	23	1.1	SSW	0.1
22	020331	2233-2324	2226-2232	5	23	0.4	W	7.8
23	020405	2230-2322	2223-2229	0	23	1.2	SSW	12
24	020407	2134-2223	2127-2133	0	22	0.7	SSW	9.8
25	020410	2248-2332	2242-2248	9	23	1.1	NE	5
26	020418	2143-2230	2137-2142	10	22	1.8	NE	8.7
27	020419	2142-2230	2135-2141	4	22	1	SSE	12
28	020423	2243-2327	2237-2243	9	23	2	NE	8.7
29	020427	2246-2329	2240-2246	9	23	0.7	SSW	6.6
30	020428	2132-2220	2125-2131	0	22	0.6	SW	9.5
31	020429	2126-2210	2120-2126	5	22	1.7	WNW	12
32	020501	2143-2228	2136-2142	0	22	1.4	SSE	5.5
33	020502	2138-2222	2132-2137	0	22	0.2	C	12
34	020503	2119-2209	2112-2118	10	22	1.5	W	11
35	020512	2153-2245	2146-2152	7	22	1.8	NE	8.3
36	020515	2143-2231	2136-2142	10	22	1.3	SW	7.3
37	020522	2149-2235	2143-2148	10	22	1.1	SSW	9.6
38	020528	2140-2228	2133-2139	6	22	0.4	SW	12.7
39	020529	2142-2228	2136-2141	4	22	1.2	SSW	7.8
40	020606	2224-2309	2218-2223	4	23	0.7	SSE	12.9
41	020608	2247-2332	2241-2246	1	23	1.6	SSW	13
42	020610	2130-2213	2124-2130	6	22	1.6	SSW	10
43	020704	2136-2224	2129-2135	9	22	1.4	SSW	10.1
44	020707	2142-2227	2135-2141	5	22	1.3	S	4.4
45	020728	2146-2232	2140-2146	---	22	0.3	WNW	5.9
46	020731	2151-2239	2144-2150	10	22	1	SSW	9.9
47	020807	2141-2225	2135-2141	0	22	1.4	SSE	12.4
48	020901	2157-2241	2150-2156	0	22	1.2	SSW	12
49	020922	2156-2241	2149-2155	10	22	1.4	SSE	1.1
50	020925	2251-2333	2245-2250	6	23	0.7	SSE	9.8
51	020926	2205-2246	2253-2258	10	22	1.6	SE	6.5
52	021002	2154-2236	2147-2153	6	22	0.8	SSE	9.9
53	021003	2133-2225	2127-2132	0	22	1.1	SE	10
54	021004	2147-2230	2141-2147	0	22	0.9	SE	9.4
55	021009	2201-2243	2155-2201	3	22	0.2	C	1.6
56	021010	2147-2228	2141-2146	0	22	0.2	C	8.7
57	021012	2146-2228	2139-2145	0	22	0.7	SE	10.3
58	021013	2137-2221	2130-2136	1	22	0.8	E	10.4
59	021014	2144-2226	2138-2143	2	22	0.1	C	5
60	021016	2147-2230	2141-2146	1	22	0.7	ESE	5.2
61	021017	2149-2232	2143-2148	0	22	0.7	SSE	8.5
62	021022	2144-2227	2138-2144	9	22	1.7	NNE	1.3
63	021024	2145-2227	2139-2144	9	22	1	SSE	7.7
64	021029	2151-2235	2142-2150	1	22	1	SSE	3.8
65	021030	2138-2218	2132-2138	1	22	0.7	ESE	1.1
66	021031	2132-2215	2125-2131	9	22	0.9	ESE	9.1
67	021106	2139-2225	2233-2138	0	22	0.7	SW	3.8
68	021112	2150-2232	2144-2150	0	22	1.5	ESE	2.7
69	021114	2143-2229	2137-2142	4	22	0.7	ESE	8.7
70	021115	2147-2227	2141-2146	5	22	0.5	SW	4.9

* include errors --- No observation NLO; Nagano Local Observatory

3.2 Other meteorological data

Meteorological data observed at the Matsushiro Observatory at the Health Center of Nagano City were used to represent the wind direction and wind speed in the study area (Fig. 1, the observatory is marked by ◎). Cloud cover was observed at point 18, where the sky was clearly visible in all directions.

3.3 Heat island intensity

We assigned points 41, 43, and 44 as urban sites, and points 14, 19, and 20 as rural sites. The calculations of *HII* were based on the averages of urban and rural temperatures (T_{u3} and T_{r3}, respectively), as follows:

$$HII = T_{u3} - T_{r3} \quad (1)$$

Urban and rural observation points were selected based on the following criteria: the scenery around the point was typical of either urban or rural scenery.

3.4 Observation of the inversion layer

Instruments attached tethered balloons can be used to take vertical temperature profiles, but such balloons can be costly and difficult to handle. Thus, the temperature distribution along a slope was used as a convenient method to obtain the vertical profile. Oke (1976) showed that the temperature along a slope agreed with the temperature of the same altitude above rural areas from observations using an aircraft and a gondola. Whiteman et al. (2004) came to the same conclusion, and referred to the temperature distribution along a steep slope as the "pseudovertical profile."

In this study, pseudovertical profiles were obtained from the temperature distributions along a steep slope based on observations from a moving car. We used 6 slope points (Z_1 to Z_6), varying in altitude from 365 m to 600 m (Fig. 1), and the bottom point Z_0, which was not written in Fig.1. Z_0 was corresponded to the lowest point in rural points 12-16 and 18-22. There were no buildings around the observation points, except for some houses near point Z_6. Points Z_1 to Z_3 were located along a stretch of orchard. Forest lined the road at points Z_4 to Z_6. Because there were no trees around each observation point on the road, the air around the point could exchange with the general air.

No time correction was done, because the maximum difference among observation periods from points Z_1 to Z_6 was within 6 min. However, the difference between observation times Z_0 and Z_1 (or Z_6) was not small and thus time correction was done.

Inversion strength denotes the vertical gradient of temperature. The vertical gradient of potential temperature was used in this study. That is the reason why the potential temperature is the conserved amount as far as there is no condensation of water vapor in the air mass. Therefore it is used as the index about the stability of the air.

4. Rural top altitude and lapse rate of the inversion layer

Figure 2 shows the averaged pattern of the pseudovertical profile based on 65 observations. The horizontal axis denotes potential temperature deviation from the ground (350 m above sea level), and the horizontal bar indicates the standard deviation. The higher the altitude, the larger the potential temperature deviation under 450 m above sea level (100 m above the ground). The gradient of potential temperature between two neighboring observation points was not constant, but larger at the lower section. The layer from 450 m to 500 m was almost under the iso-potential temperature condition. The potential temperature deviation decreased a little at 550 m, but the potential temperature reached a maximum at 600 m. Sixty five vertical temperature profiles were classified into 5 patterns at night (Table 2). There were only two nights without inversion layer. The frequency of cases that the top height of inversion layer was over 450 meters above sea level (100 meters above the ground) was more than that of other cases in fall. The highest frequency occurred in the case that the top of inversion was 365 meters above sea level (15 meters above the ground) in other seasons. It was ten to nine that inversion layer could be seen from the ground to 15 meters above the ground.

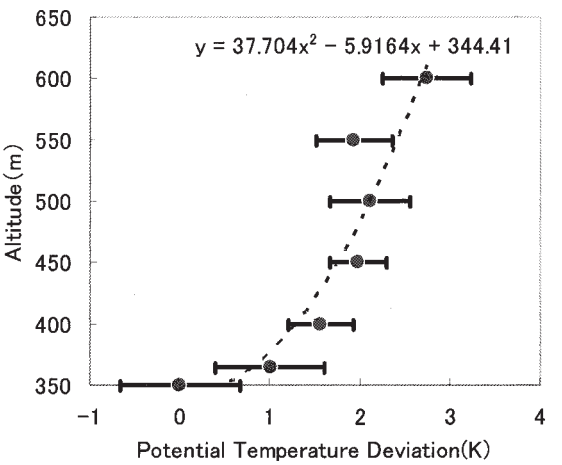

Fig. 2. Averaged pseudovertical temperature profile.
Broken line: mean values, horizontal line; standard deviation

Takechi (2000) reported that the height of the inversion top varied from 170 m to 200 m above the ground at Kochi, Japan. This range is twice as large as the result in this study. Uno et al. (1988) reported that the inversion top varied from 52 m to 130 m above the ground, with an

Table 2 Frequency of nights with an inversion layer in each season

	Non-inversion layer	Inversion layer			
		Elevated inversion	Surface inversion (ground level=350m)		
Height of inversion top			365m	400m	over 450m
Winter(Dec.-Feb.)	0	2	3	2	2
Spring(Mar.-May.)	1	0	12	7	5
Summer(Jun.-Aug.)	0	0	4	1	3
Fall(Sep.-Nov.)	1	3	4	7	8
Total	2	5	23	17	18

average of 90 m, based on tethered balloon observations at Sapporo, Japan. Whiteman et al. (2004) showed a height of approximately 100 m using tethered balloon observations and pseudovertical profiles. The results of the latter two studies agree with our results.

Next, we considered the height of the urban mixing layer at night. Because the tallest urban building had four stories, we estimated the mixing layer to be approximately 15 m. Roth (2000) reported that buildings could affect the urban atmosphere at heights 2 to 2.5 times greater than the building height. We did not unhappily observe the height of the urban mixing layer. If the result in Roth (2000) can adapt in this settlement, the height affected by a building can be 30-40 m. Thus, we regarded the potential temperature gradient between Z_0 and Z_1 as the *RLR* of the surface layer that was affected greatly by buildings.

5. Temperature anomaly distribution on fine and cloudy days

We selected 49 cases to study the average temperature distribution for fine days. We calculated the average temperature of all observation points (n = 48) for each case, and the temperature anomaly of each point. Figure 3a shows the distribution of the average temperature anomaly. A warmer zone appeared around points 41 and 45, and a colder zone occurred around points 4, 5, 14, 15, and 19 in rural areas.

Figure 3b shows the average temperature anomaly distribution on 18 cloudy days. The pattern of cloudy days was similar to that of fine days, but the temperature difference between the warm and cold zones for cloudy days was smaller than that for fine days. On

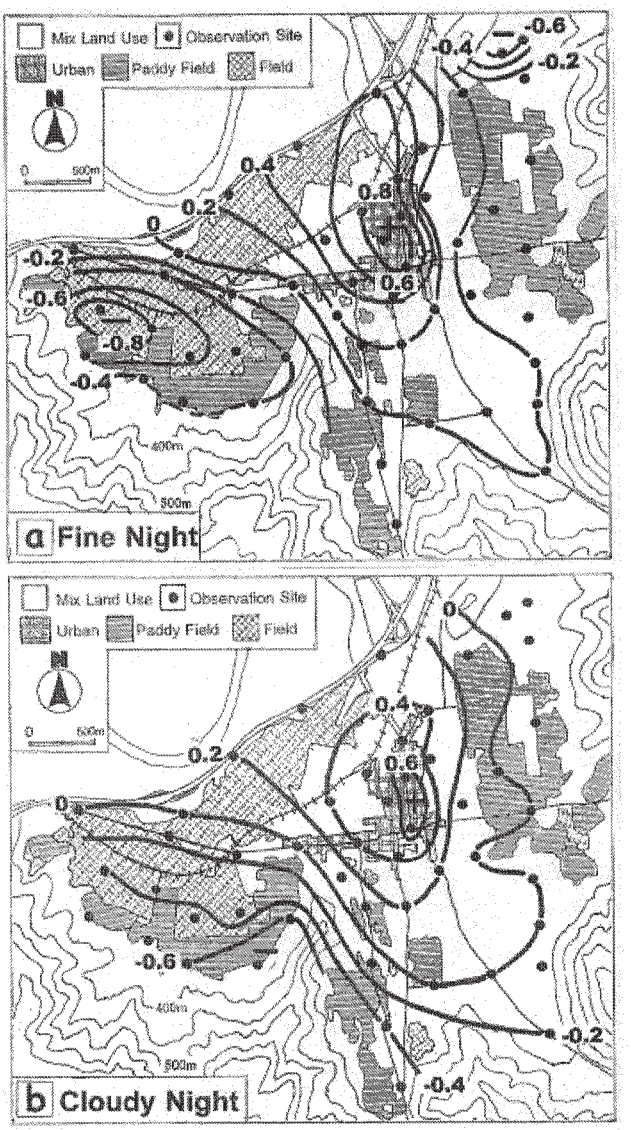

Fig. 3. Average temperature anomaly distribution on fine and cloudy nights.

cloudy days, the cold zone was not in the center of the field area but at points 21 and 22 near the foot of the mountain.

6. Rural lapse rate, heat island intensity, and meteorological conditions

We studied how *HII* and *RLR* changed with meteorological conditions, such as wind speed and cloud cover, using 63 temperature surveys that included both vertical and cloud cover observations. Figure 4 shows the relationship between *HII* and wind speed. No cases of strong wind occurred during these observations. C denotes the cloudiness. When the sky is perfectly covered by cloud, cloudiness is corresponded to 10. Generally speaking, the smaller the wind speed, the greater the *HII*. But the maximum of *HII* reached at a wind speed of 0.7 m/s. As cloud cover decreased, *HII* increased.

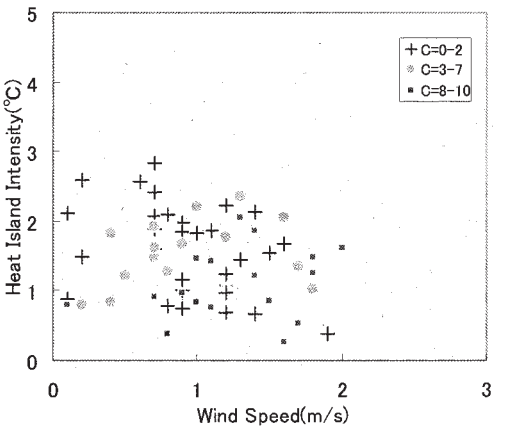

Fig. 4. Relationship between wind speed and heat island intensity.

Figure 5 shows the relationship of *RLR* to wind speed. The smaller the wind speed, the greater the lapse rate, too. However, the *RLR* did not simply become small as wind speed increased. The maximum of *RLR* occurred at a wind speed of 0.7 m/s, suggesting that nocturnal heat island formation is controlled partly by mechanically generated turbulence from the city roughness rather than by anthropogenic heat alone. Furthermore, less cloud cover resulted in a greater *RLR*.

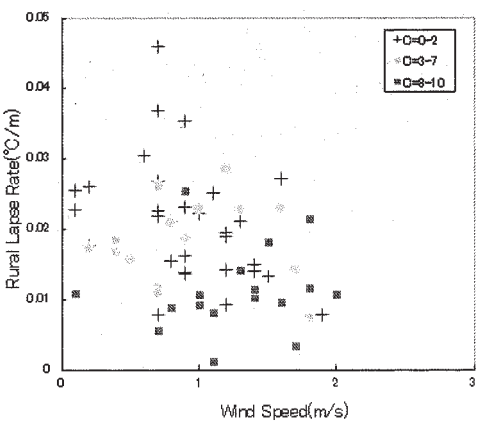

Fig. 5. Relationship between wind speed and the rural lapse rate.

The association of less cloud cover with a larger *HII* can be explained as follows. First, urban areas had a smaller sky view factor than did rural areas. When there was little cloud cover, rural areas cooled more than urban areas at night. Both urban areas and rural areas experienced little cooling on cloudy nights. The *HII* depended on rural cooling, which was more affected by cloud cover than was urban cooling.

The *RLR* was proportional to the difference between the surface temperature and the temperature at some higher level. Because the temperature at higher levels has a small effect on

surface conditions, the *RLR* depends on surface cooling. Briefly, both *HII* and the *RLR* can be largely determined by the rural surface temperature. Therefore we should study rural information such as soil temperature, the exposure of soil, water content in the soil and so on to clarify heat island formation.

Next, we examined why the maximums for *HII* and *RLR* did not simply become small as the wind speed increased. Maximum values were considered to represent conditions in which factors except wind speed acted ideally in regard to *HII* and *RLR*. The surface cooled well during calm, clear nights. At higher wind speeds, the air on the ground mixed with the air at higher levels, resulting in little surface cooling.

However, at some wind speeds, radiative cooling proceeded, and an inversion layer developed in rural areas. The air on the ground mixed with the warmer air above the urban area, resulting little cooling of the urban surface. Consequently, we considered the maximum *HII* to occur at the same specific wind speed.

Figure 6 shows the relationship between *HII* and *RLR* using the 65 data points. The regression of *RLR* and *HII* is given by:

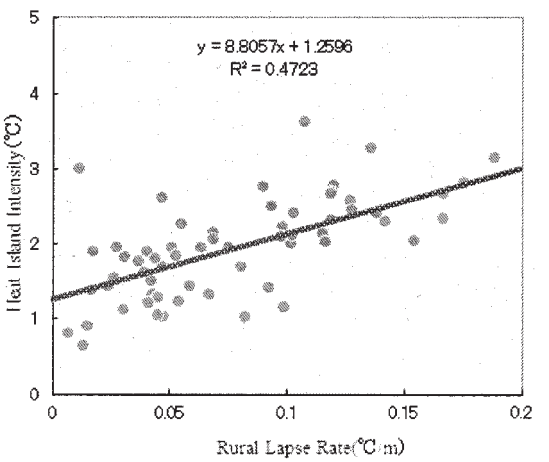

Fig. 6. Relationship between the rural lapse rate and heat island intensity.

$$HII = 8.8057 \times RLR + 1.2596 \quad (2)$$

The coefficient of correlation is 0.69. The *RLR* of the surface layer accounts for the *HII*, and statistically confirms that a large *RLR* is associated with a large *HII*.

Some cases had a nonlinear pseudovertical profile from the ground to 100 m. The estimation of *RLR*, which is the gradient of the linear regression of vertical profiles, requires consideration. Some problems affected this estimation, including how to determine *RLR*, because the smaller the height the larger the *RLR*, and the height of the inversion top was not always 100 m; also, the pseudovertical profiles had a mean cold temperature bias of about 0.4℃, compared to free air within the basin, with a standard deviation of about 0.4℃ (Whiteman et al., 2004). Further study of how these factors influence *RLR* estimation should be conducted.

7. Discussion

Figure 7 compares the relationship between *HII* and *RLR* found in this study with results from previous reports (Ludwig, 1974; Tamiya and Ohyama, 1981). The Small, Middle, and Large denoted on the regression line represent cities of different sizes studied by Ludwig (1974). Ludwig classified observational data into those three groups as follows: Small (pop. 33,000-270,000), Middle (pop. 360,000-790,000), and Large (pop. 835,000-2,270,000) cities. Ludwig showed the regressions between *HII* and *RLR* for these categories. Note that the unit of the horizontal line (℃/hPa) differs from that of Figure 6.

From the equation of state, the hydrostatic equation is given as:

$$\Delta p/\Delta z = -p g/(RT), \quad (3)$$

where p, g, R, T, and z denote the pressure, gravitational constant, gas constant, air temperature, and height, respectively. As noted above, the altitude of Matsushiro Town is about 350 m. In the case of p = 960 hPa, T = 288 K, g = 9.8 m/s^2, and R = 287 JK^{-1}Kg^{-1},

$$\Delta p/\Delta z = 0.1138 \quad (\text{hPa/m}) . \quad (4)$$

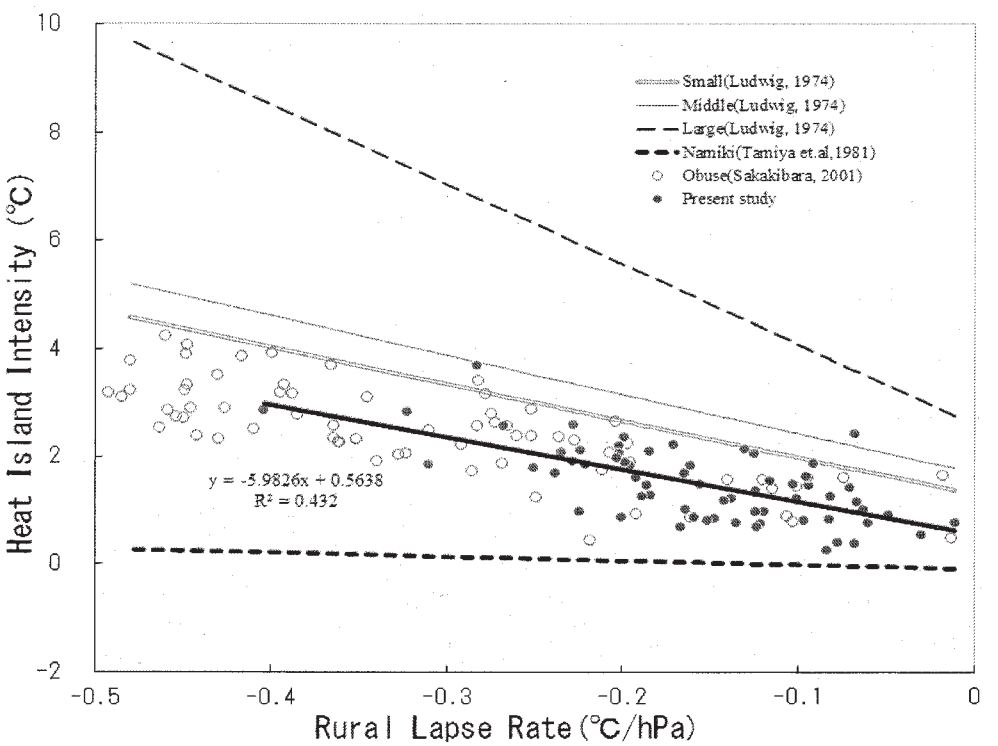

Fig. 7. City size and regression between the rural lapse rate and heat island intensity.

We converted the unit of the horizontal axis into °C/hPa by dividing this value into *RLR*.

Matsushiro has a population of approximately 20,000, which is smaller than the small city classification by Ludwig (1974). Previous studies have examined Obuse, Nagano, Japan, which had almost the same population as Matsushiro (Sakakibara, 2001) and Takezono, Tsukuba, Ibaraki, Japan, which was smaller than Matsushiro with a population of 1,300 (Tamiya and Ohyama, 1981). To convert to °C/hPa for Obuse, we used the same value for $\Delta p/\Delta z$ as for Matsushiro, because Obuse is located near Matsushiro. For Takezono we used the value of $\Delta p/\Delta z$ with p of 1013 hPa for Equation (3).

Almost all of the plots for Matsushiro fell under the regression line of Ludwig's 'Small' category, and above the regression line for Takezono. Plots for Matsushiro slightly overlapped those for Obuse. Thus our results show that the relationship between *HII* and *RLR* presented by Ludwig (1974) can be extended in smaller cities.

8. Conclusions

This study examined temperature distributions observed along a steep slope in and around Matsushiro Town, Nagano, Japan, and the relationship between *HII* and rural lapse rate (*RLR*). More cloud cover and higher wind speeds both resulted in smaller *HII* and *RLR* values. Heat islands and rural inversion layers formed under the same meteorological conditions. The maximums of *HII* and *RLR* were also the largest at a wind speed of 0.7 m/s. This suggests that nocturnal heat island formation is controlled partly by mechanically generated turbulence caused by urban roughness rather than solely by anthropogenic heat. There was a high correlation between *HII* and *RLR* in the settlement, and Ludwig's classification system can apply to smaller cities. Because city size does not directly influence *RLR*, the mixing depth of large cities may be higher than that of small cities. More extensive field observations, including vertical soundings in both rural and urban stations and measurements about rural conditions must be conducted.

Acknowledgments

We thank the Health Center of Nagano for providing us with meteorological data. Special thanks are due to Mr. Takashi Hamada of the Nagano Environmental Conservation Research Institute for helpful comments on this paper.

References

Kusaka, H., and Kimura, F., 2004: Thermal effects of urban canyon structure on the nocturnal heat island: numerical experiment using a mesoscale coupled with an urban canopy model.

J. Appl. Meteor., **43**, 1899-1910.

Ludwig, F.L., 1974: Urban temperature fields. *"Urban Climates" WMO Publ Tech Note,* **108**, 80-112.

Oke, T.R., 1973: City size and the urban heat islands. *Atmospheric Environment*, **7**, 769-779.

Oke, T.R., 1976: The distinction between canopy and boundary-layer urban heat islands. *Atmosphere*, **14**, 268-277.

Roth, M., 2000: Review of atmospheric turbulence over cities. *Quart. J. of Roy. Meteor. Soc.*, **126**, 941-990.

Sahashi, K. 1983: Errors in the air temperature observation by traveling method with the automobiles-Effects of the automobiles. *Tenki*, **30**, 509-514 (in Japanese).

Sakakibara, Y., 1998: The relationship between windspeed and/or ground inversion strenth over rural environs and nighttime urban heat island intensity in Nagano city. *Tenki*, **45**, 119-120.

Sakakibara, Y., 2001: Comparison between the effect of heating from urban surface and that of mechanical mixing of urban atmosphere to heat island. *Tenki,* **48**, 305-311. (in Japanese).

Summers, P.W., 1965: An urban heat island model; its role in air pollution problems, with applications to Montreal. *Paper presented to "First Canadian Conference on Micrometeorology" in Toronto 12-14 April*, 32 pp.

Takechi, N., 2000: A Study of the ground inversion and the heat island intensity in Kochi city. *Geographical Science*, **55**, 99-106. (in Japanese).

Tamiya, H., and Ohyama, H., 1981: Nocturnal heat island of small town, its manifestation and mechanism. *Geographical Review of Japan*, **54**, 1-21. (in Japanese).

Uno, I., Wakamatsu, S., and Ueda, H., 1988: An observational study of the structure of the nocturnal urban boundary layer. *Boundary-Layer Meteor.*, **45**, 59-82.

Whiteman, C.D., Eisenbach, S., Pospichal, B., and Steinacker, R., 2004: Comparison of vertical soundings and sidewall air temperature measurements in a small alpine basin. *J. Appl. Meteor.*, **43**, 1635-1647.

(2011年10月11日　受付)
(2012年１月20日　受理)